



Thermodynamical and Microstructural SME Study on CuAlNi and CuAlNiCo Shape Memory Alloys

^{1*}Canan Aksu Canbay, ²Güneş Başbağ, ¹Oktay Karaduman, ²Mustafa Boyrazlı

¹FiratUniversity, Faculty of Science, Department of Physics, Elazig 23169, Turkey

²Department of Metallurgical and Materials Engineering, Engineering Faculty, Firat University, Elazig, Turkey

In this work, Cu-Al-Ni and Cu-Al-Ni-Co shape memory alloys were fabricated by arc melting process under vacuum. The fabricated samples were cut from the ingot into small pieces. After then, the samples homogenized and thermal and structural observations were made by DSC, TG/DTA and X-ray equipments. As the heating/cooling rate changed, the transformation temperatures were changed slightly. On the left side of heating parts of the cycles, the first downward endothermic peaks belong to the forward M→A transformation where $\beta 1'$ converts to $\beta 1$ (L21) phase. Then, the α and $\gamma 2$ precipitation phases emerge and dissolute and convert to a stable ordered $\beta 2$ phase which can be understood from the downward eutectoid dissolution peaks.

Keywords: Cu-Al-Ni, Cu-Al-Ni-Co, Shape memory alloys, Martensite, DSC, DTA, X-ray diffraction

Submission Date: 10 December 2020

Acceptance Date: 08 January 2021

*Corresponding author: caksu@firat.edu.tr

1. Introduction

Nowadays, smart materials and structures or smart material systems have been receiving ever increasing attention because of their great scientific and technological importance [1, 2]. One of the most functional class among smart materials is shape memory alloys [2]. Shape memory alloys (SMAs) are made up of metal elements and first discovered by A. Olander in 1938 [1, 3]. SMAs exhibit very important and beneficial properties as shape memory effect (SME), and pseudo-elasticity (PE).

Shape memory effect (SME) is one of the fantastic behaviors of SMAs such that they return back to their original shape by heating them after been deformed mechanically. SME is performed through an isothermal and

diffusionless solid-solid phase transition in these materials [4]. This reversible phase transition occurs between martensite and austenite phase of SMAs is called as martensitic transformation. In SMAs, transformation of the martensite phase to the austenite phase is generally defined as thermo-dynamic cycle [2]. The austenite phase is also defined as high temperature or parent phase and martensite phase is called as low temperature or product phase. SME can be one way shape memory effect (OWSME) and two way shape memory effect (TWSME). In one way shape memory effect, SMAs in deformed martensite phase change their shape to the original shape upon heating but after then they do not return to the deformed shape by cooling again. However, in the case of two way shape memory effect (this

property is provided in SMAs by performing some special post treatments on these alloys), SMAs can return to deformed shape (cold temperature shape) by cooling them when they are in austenitic shape (hot temperature shape) at austenite phase, they will automatically deform without any external deformation [5].

Another amazing property of SMAs is pseudoelasticity (PE) or superelasticity (SE). SE refers to characteristic that certain materials possess. SE materials can return to their original shape when the applied deformational stress is removed [6]. SMAs can behave superelastic when they are in austenite phase.

Generally SMAs consist of 3 structures. These structures are NiTi (and NiTi-based), Cu-based and Fe-based SMAs [7] which have been found to be commercially attractive. Cu-based alloys are nearly ten times cheaper than the NiTi(-based) SMAs which have superior SMA properties and are the most dominant among SMAs even today [2, 7-9]. Therefore, Cu-based SMAs have received a considerable attention, also for their high damping and thermal stability [10]. However, the polycrystalline copper based SMAs, such as Cu–Al–Ni and Cu–Zn–Al, are too brittle and cannot, therefore, be cold worked due to the high degree of order and high elastic anisotropy that exist in the parent austenitic β –phase [11]. To reduce brittleness by grain size refinement and improve ductility, Cu-based binary and ternary systems can be doped by some grain refining elements such as Ti, Co, Zr, B, Fe, or Cr [3, 7, 8, 11, 12].

2. Experimental

The ternary 80.6Cu-15.74Al-3.67Ni (at.%) and quaternary 79.41-14.1Al-5.19Ni-1.3Co (at.%) polycrystalline shape memory alloys were produced by using high purity (99.9%) elements of copper, aluminum, nickel and cobalt powders. After mixing the powders as to the alloys' compositions, the pelletization was made under pressure. The pellets were melted by an Edmund Buehler Arc Melter under inert argon atmosphere and thus the alloys were obtained as cast ingots. Then, the undersized (~30-50 mg) slab shaped specimens of alloys were cut from these ingots then all of these samples were solution-treated in β - phase region and without delay

they were quenched into iced-brine water to make the formation of $\beta 1'$ martensite phase in the alloys' matrices.

The chemical compositions of alloys as atomic percentages (at.%) were determined by a Zeiss Evo MA10 model EDX (energy dispersive X-ray) instrument at room temperature. The characteristic martensitic transformation peaks and analyzed data for each alloy were obtained by using a Shimadzu DSC-60A model differential scanning calorimetry (DSC) equipment run at different heating/cooling rates of 15, 20, 25, 30 and 35 °C/min. The high temperature β -phase region was observed by means of a Shimadzu DTG-60AH model differential thermal analysis (DTA) instrument run at a single heating rate of 25 °C/min for each alloy from room temperature to 900 °C. The X-ray measurements (with $\text{CuK}\alpha$ radiation) at room temperature were performed by a Rigaku RadB-DMAX II diffractometer to expose the diffraction peaks of lattice planes of the alloys.

3. Results

The DTA heating curves of the CuAlNi and CuAlNiCo alloys can be seen in Fig.1 and Fig.2. As seen in these figures, a multiple phase transition sequence of $\beta 1' \rightarrow \beta 1(\text{DO}_3 \text{ or } \text{L}2_1) \rightarrow \beta 2(\text{B}2) \rightarrow \alpha + \gamma 2 \text{ precipitation} \rightarrow \text{eutectoid dissolution} \rightarrow \beta 2(\text{ordered A}1) \rightarrow \text{A}2(\text{disordered})$ starting from the far left to the far right was observed. This characteristic batch of phase transitions is common to the Cu-Al based SMAs [3, 4, 7, 12-16]. However, it is seen that the forward $\beta 1'$ martensite to $\beta 1$ austenite ($\text{M} \rightarrow \text{A}$) transformation, which is the sign of SME property of SMAs, occurred more powerful (i.e. with deeper endo peak) for CuAlNiCo alloy (as seen in Fig.2) than that of CuAlNi alloy (Fig.1). The addition of Co and increased percentage of Ni caused this improvement for the CuAl base alloys with almost same compositions used in this work. This is also the reason for that the eutectoid peak seen more shallow for CuAlNi alloy with a slightly higher Cu content that contributed to this result. In other words, the sharper eutectoid peak, the better alloying.

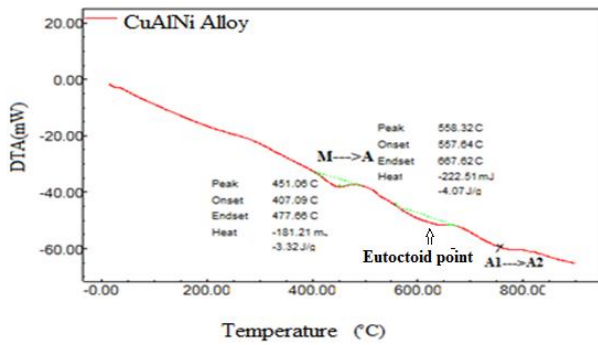


Figure.1. The DTA curve of CuAlNi alloy at the single heating rate of 25 °C/min.

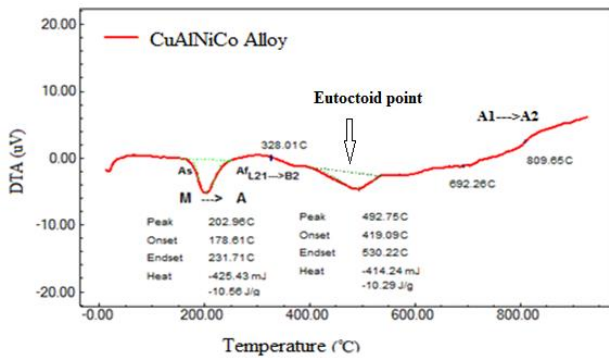


Figure.2. The DTA curve of CuAlNiCo alloy at the single heating rate of 25 °C/min.

Among the data sets of analyzed M→A transformation peaks displayed under the M→A peaks of DTA curves, the given onset, endset, and peak temperatures are the austenite-start (A_s), -finish (A_f), and -max (A_{max}) temperatures, respectively. As seen from these data sets, both two alloys should be classified as high temperature shape memory alloys due to their A_f temperatures were found above 100 °C [17, 18].

The cyclic DSC heating/cooling curves of the alloys can be seen in Fig.3 and Fig.4. The characteristic M→A transformation temperatures (A_s , A_f and A_{max}) and enthalpy change ($\Delta H_{M\rightarrow A}$) values of the alloys for M→A transition peaks were obtained by doing DSC peak analyses made on these peaks and are given in Table 1 and Table 2. The transformation temperatures and enthalpy change ($\Delta H_{M\rightarrow A}$) values seen from these tables are seen to be changed by different heating/cooling rates and they also some differed from the values given in data sets of the analyzed DTA curves. On the heating fragments of the DSC curves, there exist several variously sized head-down endothermic peaks

of the forward M→A transformations seen at between ~300-450 °C for CuAlNi (in Fig.3) and at ~200-300 °C for CuAlNiCo (in Fig.4) alloys where $\beta 1'$ martensite phase changes to $\beta 1$ ($DO_3/L2_1$) austenite phase [12-18]. On DSC curves of the alloys, none of the backward A→M transformation peaks and also some of forward M→A transformation peaks on heating fragments of some curves run at slow DSC heating/cooling rates are not observed due to the low heating rates and slow cooling ability of the used DSC instrument. Moreover, there are seen thermal lag (temperature lagging) which occurred on the heating parts of the curves of CuAlNi alloy (in Fig.3) run at 30 and 35 °C/min of heating rates due to these high heating rates and also due to the geometry of tested CuAlNi alloy sample and its morpho-touching on the base layer of DSC crucible where the test sample is put in. A detailed explanation of such kinds of lagging temperature problems can be found in a recent work [9].

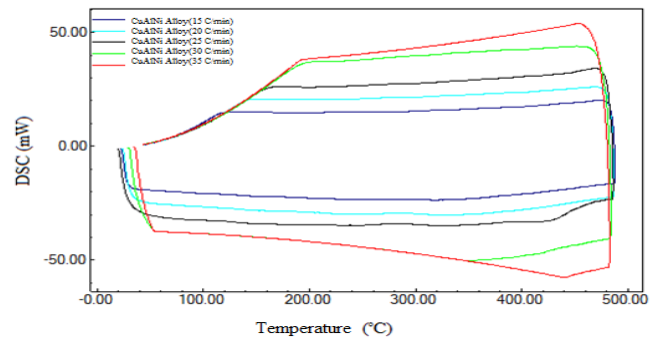


Figure 3. The DSC curves obtained for CuAlNi alloy for heating at the heating/cooling rates of 15, 20, 25, 30, and 35 °C/min.

Table.1. The forward M→A transformation temperatures and enthalpy change values for the CuAlNi alloy obtained by DSC peak analyses.

Heating Rate	A_s (°C)	A_f (°C)	A_{max} (°C)	$\Delta H_{A\rightarrow M}$ (J/g)
15	290,01	375,30	320,52	2,90
20	208,32	274,69	245,03	1,10
25	286,68	386,26	333,00	2,09
35	317,64	417,17	348,03	4,76
45	417,71	458,66	441,60	1,57

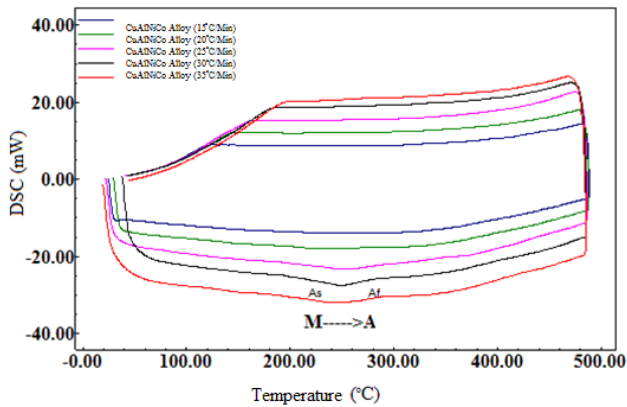


Figure 4. DSC curves obtained for CuAlNiCo alloy at the heating/cooling rates of 15, 20, 25, 30, and 35 °C/min.

Table.2. The forward M→A transformation temperatures and enthalpy change values for the CuAlNiCo alloy obtained by DSC peak analyses.

Heating Rate	As(°C)	Af(°C)	Amax(°C)	$\Delta H_{A \rightarrow M}$ (J/g)
15	209,37	266,01	245,36	1,90
20	177,36	281,78	233,57	3,54
25	201,33	287,44	253,20	6,28
30	208,75	277,61	249,09	6,27
35	222,08	283,24	261,83	2,61

Furthermore, as seen in Table 1 and Table 2, the M→A transformation temperatures of the alloys were generally increased by increase of heating/cooling rate. But, they were found lower for CuAlNiCo alloy than for CuAlNi alloy due to the Co addition, and high copper content in CuAlNi alloy led it to have higher transformation temperatures (in Table 1).

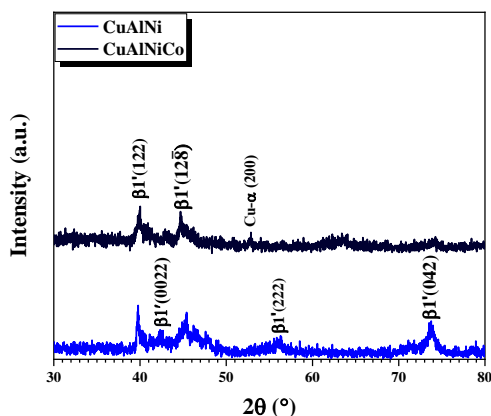


Figure 5. The XRD results for CuAlNi and CuAlNiCo alloys showing different planes of β_1' martensite phase.

The results of XRD measurements of the alloys performed at room temperature are given in Fig.5. According to these X-ray diffraction patterns, the highest main peak indicates the β_1' (122) martensite phase and the other appearing

peaks are β_1' (0022), β_1' (128 $\bar{}$), β_1' (222), and β_1' (042) martensites and a Cu- α (200) precipitation peak [3, 4, 7, 12, 16-18]. Among these peaks, the intensities of β_1' (222), and β_1' (042) lowered by the addition of Co addition into CuAlNi alloy. But due to the lower Al content and Co addition the intensity of Cu- α (200) precipitation peak arrived on the scene on the diffraction pattern of CuAlNiCo alloy.

4. Conclusions

In this work Cu-Al-Ni and Cu-Al-Ni-Co high temperature shape memory alloys were successfully produced by arc melting. The phase transformation from martensite to austenite observed on both DSC and DTA curves of the produced alloys indicated the SME property of the alloys. It is found that each one of two alloys is a high temperature shape memory alloys due to that their A_f temperatures were observed above 100 °C. The high transformation temperatures caused by high Cu content of CuAlNi alloy reduced by the Co addition. The DTA curves revealed a multiple phase transition sequence of $\beta_1' \rightarrow \beta_1$ (DO₃ or L2₁) $\rightarrow \beta_2$ (B2) $\rightarrow \alpha + \gamma_2$ precipitation \rightarrow eutectoid dissolution $\rightarrow \beta_2$ (ordered A1) \rightarrow A2(disordered) that occurred in both alloys as this is common to the CuAl-based alloys. Furthermore, the microstructural X-ray measurements showed that both alloys predominantly have β_1' martensite with varied orientations at room temperature.

References

- [1] Özkul, İ., Kurgun, M. A., Kalay, E., Canbay, C. A., & Aldaş, K. (2019). Shape memory alloys phenomena: classification of the shape memory alloys production techniques and application fields. *The European Physical Journal Plus*, 134(12), 585. <https://doi.org/10.1140/epjp/i2019-12925-2>
- [2] Kim, W. C., Lim, K. R., Kim, W. T., Park, E. S., & Kim, D. H. (2020). Recent advances in multicomponent NiTi-based shape memory alloy using metallic glass as a precursor. *Progress in Materials Science*, 100756. <https://doi.org/10.1016/j.pmatsci.2020.100756>
- [3] Canbay, C.A., Genc, Z.K. & Sekerci, M. Thermal and structural characterization of Cu–Al–Mn–X (Ti, Ni) shape memory alloys. *Appl. Phys. A* 115, 371–377 (2014). <https://doi.org/10.1007/s00339-014-8383-6>
- [4] Canbay, C.A., Bakır Bazlı Şekil Hatırlamalı Alaşım Üretimi ve Alaşımın Yapısal, Termal ve Elektriksel Özelliklerinin İncelenmesi, (2010), Doktora Tezi, Fırat Üniversitesi, Fen Bilimleri Enstitüsü, Elazığ
- [5] Lexcellent, C., Leclercq, S., Gabry, B., & Bourbon, G. (2000). The two way shape memory effect of shape memory alloys: an experimental study and a phenomenological model. *International Journal of Plasticity*, 16(10-11):1155-1168. [https://doi.org/10.1016/S0749-6419\(00\)00005-X](https://doi.org/10.1016/S0749-6419(00)00005-X)
- [6] Anand, L., & Gurtin, M. E. (2003). Thermal effects in the superelasticity of crystalline shape-memory materials. *Journal of the Mechanics and Physics of*

- Solids, 51(6), 1015-1058. [https://doi.org/10.1016/S0022-5096\(03\)00017-6](https://doi.org/10.1016/S0022-5096(03)00017-6)
- [7] Canbay, C. A., Karaduman, O., & Özkul, İ. (2019). Investigation of varied quenching media effects on the thermodynamical and structural features of a thermally aged CuAlFeMn HTSMA. *Physica B: Condensed Matter*, 557, 117-125. <https://doi.org/10.1016/j.physb.2019.01.011>
- [8] Al-Humairi, S. N. S. (2019). Cu-based shape memory alloys: modified structures and their related properties. *Recent Advancements in the Metallurgical Engineering and Electrodeposition*.
- [9] Canbay, C.A., Karaduman, O. & Özkul, İ. Lagging temperature problem in DTA/DSC measurement on investigation of NiTi SMA. *J Mater Sci: Mater Electron* 31, 13284–13291 (2020). <https://doi.org/10.1007/s10854-020-03881-y>
- [10] Raju, T.N., Sampath, V. Effect of Ternary Addition of Iron on Shape Memory Characteristics of Cu-Al Alloys. *J. of Materi Eng and Perform* 20, 767–770 (2011). <https://doi.org/10.1007/s11665-011-9916-1>
- [11] Lojen, G., Gojić, M., & Anžel, I. (2013). Continuously cast Cu–Al–Ni shape memory alloy– Properties in as-cast condition. *Journal of Alloys and Compounds*, 580, 497-505. <https://doi.org/10.1016/j.jallcom.2013.06.136>
- [12] Karaduman, O., Özkul, I., Altın, S., Altın, E., Bağlayan, Ö., & Canbay, C. A. (2018, November). New Cu-Al based quaternary and quinary high temperature shape memory alloy composition systems. In *AIP Conference Proceedings* (Vol. 2042, No. 1, p. 020030). AIP Publishing LLC. <https://doi.org/10.1063/1.5078902>
- [13] S.M. Chentouf, et al., Microstructural and thermodynamic study of hypoeutectoidal Cu–Al–Ni shape memory alloys. *Journal of Alloys and Compounds*, Vol 470: pp.507–514, (2009). <https://doi.org/10.1016/j.jallcom.2008.03.009>
- [14] O. Karaduman et al., Analysis of a newly composed Cu-Al-Mn SMA showing acute SME characteristics. *AIP Conference Proceedings* 2178, 030039 (2019); <https://doi.org/10.1063/1.5135437>
- [15] C.A. Canbay, M. Ali Çiçek, Oktay Karaduman, İskender Özkul, Memet Şekerci. (2019). Investigation of Thermoelastical Martensitic Transformations and Structure in New Composition of CuAlMnTi Shape Memory Alloy. *JOURNAL OF MATERIALS AND ELECTRONIC DEVICES*, 1(1), 60-64. Retrieved from <http://dergi-fytronix.com/index.php/jmed/article/view/45>
- [16] Karaduman, O.; Aksu Canbay, C.; Özkul, İ.; Aziz Baiz, S.; Ünlü, N. Production and Characterization of Ternary Heusler Shape Memory Alloy With A New Composition. *J. mater. electron. device*. 2018, 1, 16-19. <http://dergi-fytronix.com/index.php/jmed/article/download/24/72>
- [17] Karaduman, O., Ünlü, N., Canbay, C. A., Özkul, İ., & Baiz, S. A. (2018). The Investigation of SME in a Cu-Al-Ni HTSMA. *JOURNAL OF MATERIALS AND ELECTRONIC DEVICES*, 1(1), 6-10. <http://dergi-fytronix.com/index.php/jmed/article/view/22>
- [18] Canbay, C. A., Karaduman, O., Ünlü, N., Baiz, S. A., & Özkul, İ. (2019). Heat treatment and quenching media effects on the thermodynamical, thermoelastical and structural characteristics of a new Cu-based quaternary shape memory alloy. *Composites Part B: Engineering*, 174, 106940. <https://doi.org/10.1016/j.compositesb.2019.106940>